

Experimental demonstration of radiation flux measurement accuracy surpassing the Nyquist limit

Richard Lieu¹, Michael Stefszky², T.W.B. Kibble³, and Johann, C. -H. Shi⁴

¹*Department of Physics, University of Alabama, Huntsville, AL 35899*

²*Integrated Quantum Optics, University of Paderborn, Warburger Strasse 100, 33098 Paderborn, Germany.*

³*Blackett Laboratory, Imperial College, London SW7 2AZ, U.K.*

⁴*Astrophysics Center, Department of Physics, Tsinghua University, Beijing, China.*

ABSTRACT

In this paper we present an extensive and detailed experimental assessment of the performance of homodyne detection vs direct detection for determining the flux of an incoherent light source. The intensity of a laser reference signal is measured, before and after contamination by photon bunching noise (transimpedance gain of 20k), simultaneously. Moreover, the measurement containing photon bunching noise was done using two schemes: direct and homodyne detection, also with no appreciable time delay. The sampling rate of all measurements is the same, and is always higher than the frequency limit of the bunching noise. By carefully comparing the resulting three time series, it is found, surprisingly, that the homodyne detection of the incoherent signal resembles more closely the variance and variability pattern of the original coherent signal, and the effect is most prominent at the highest sampling frequency. It therefore appears flux estimates made using the shot noise of the field were able to overcome the Nyquist theorem, *viz.* by combining the homodyne technique with sampling at a rate faster than the bunching noise fluctuations it is possible to surpass the sensitivity limit of the radiometer equation. This is, to the best of our knowledge, the first time that such a detailed analysis of shot noise fluctuations has been investigated experimentally. Although a full theoretical understanding is still lacking, the experiments appear to show an unambiguous effect that requires further investigation.

1. Introduction

Recently, Lieu et al (2015a) proposed a method of improving the sensitivity of radio telescopes beyond the limit set by the radiometer equation, using a 50:50 beam splitter

and measuring the difference signal between the two output beam intensities. The original motivation of Lieu et al (2015a) was based upon the supposition that the intensity difference has shot noise fluctuations given by a simple Poisson process with its mean subtracted away, and a variance equal to the mean photon rate of the (presumed stationary) incident beam. The statistics of the noise distribution presented in Lieu et al (2015a) were derived from the quantum theory of chaotic light. Subsequently, it was revealed by Zmuidzinas (2015) that the higher moments of Lieu et al (2015a) were erroneous, due to an invalid assumption about the absence of correlations between non-overlapping time intervals. Recently, a simplified calculation that reaches the same conclusion as Zmuidzinas (2015) was presented by us in Lieu & Kibble (2015b). In essence, we showed (after correcting the mistake in Lieu et al (2015a)) that although it is possible to use the split-beam technique to achieve about the same accuracy as that of a direct measurement of the incoming signal, it is impossible to do better. Although the three aforementioned papers assumed the light signal is stationary, Nair & Tsang (2015) developed a general theorem that limits the sensitivity of any method of detecting any light signal of high occupation number to that of the classical radiometer equation.

It may be useful to seek a heuristic understanding of the difference between Lieu et al (2015a) and the three subsequent papers cited above. If light comprises only shot noise, the fluctuations in direct and homodyne measurements will in principle both look the same. But, as is usually the case for chaotic light, there are classical phase noise fluctuations as well, and the shot noise will then exhibit a time dependent mean and variance as its amplitude varies together with the classical intensity noise in tandem. According to Zmuidzinas (2015); Lieu & Kibble (2015b); Nair & Tsang (2015), this correlation between the shot noise variance and the classical noise intensity is not expected to be removed by the beam splitter, as illustrated in Figure 1. Lieu et al (2015a), on the other hand, suggested that the appearance of the balanced homodyne difference signal remains like simple shot noise with the mean subtracted away.

In this paper we present a real experimental comparison between the accuracy limits of a homodyne measurement and a direct measurement of an incoherent light field. The results indicate, contrary to the expected outcome, that the homodyne measurement *did* indeed provide a significant accuracy enhancement over the direct measurement, although not at the very optimistic level first envisaged by Lieu et al (2015a) which treated the higher moments of the field operators incorrectly. If the effect is due to the specific experimental conditions, then these results might still lead to methods or observational scenarios beneficial to radio astronomy in some way. On the other hand, if the experimental conditions did match in every way the ansatz of the theoretical prediction, which to the best of our current understanding seems to be the case, then the apparent contradiction between our data and

the calculations of Zmuidzinas (2015); Lieu & Kibble (2015b); Nair & Tsang (2015) would represent a fundamental paradigm shift from standard quantum field theory that occurs at high orders of field operators (precisely 8th order and upwards).

2. The experiment

In the previous section we discussed recent quantum optics calculation as an extension of earlier semi-classical treatment of n -point correlation functions in which the amplitudes are classical c -numbers (*e.g.* Wang et al (1989)). Although the results appear theoretically sound, there are possibly already hints of disagreement with observation of laser intensity fluctuations. Thus, it has been found that classical noise can be reduced by the technique of optical homodyne detection wherein the vacuum serves as the signal field and the field of interest is the local oscillator, see *e.g.* Stefszky et al (2012). This setup is therefore equivalent to the aforementioned beam splitter detection, followed by the exclusion of low frequencies, to produce shot noise of sufficient stability to exhibit a linear relationship between noise power and photocurrent intensity, Fox (2006). In fact, such a setup was even used as random number generator, as the Fourier spectrum of the subtracted intensity has the qualifying property, *viz.* an autocorrelation function comprising a narrow central spike above a zero background, Shen et al (2010).

In this section the experiment, we discuss specifically tests of the key predictions of section 1. Our test consists of two main parts: correlation functions, and the accuracy of flux measurements. First, however, we describe the experiment itself in some detail.

2.1. Basic setup

An overview of our measurement setup is shown in Figure 2. There are three key components to this setup: the low noise fiber laser that provides a stable reference field, the rotating glass plate used to produce pseudo-thermal light from this laser, and the simultaneous detection of a reference field and the homodyne and direct detection of the pseudo-thermal light.

The laser is a highly stable 1 Watt 1550nm RIO Grande laser system which includes a low-noise erbium doped fibre amplifier. The output of the laser is attenuated in order to remove as much of the excess noise due to amplification as possible. The RIN (relative intensity noise) characteristics of the laser (specified at 1 mW) show that the laser intensity is shot-noise limited by about 40 kHz and the linewidth of the laser is less than 1 kHz.

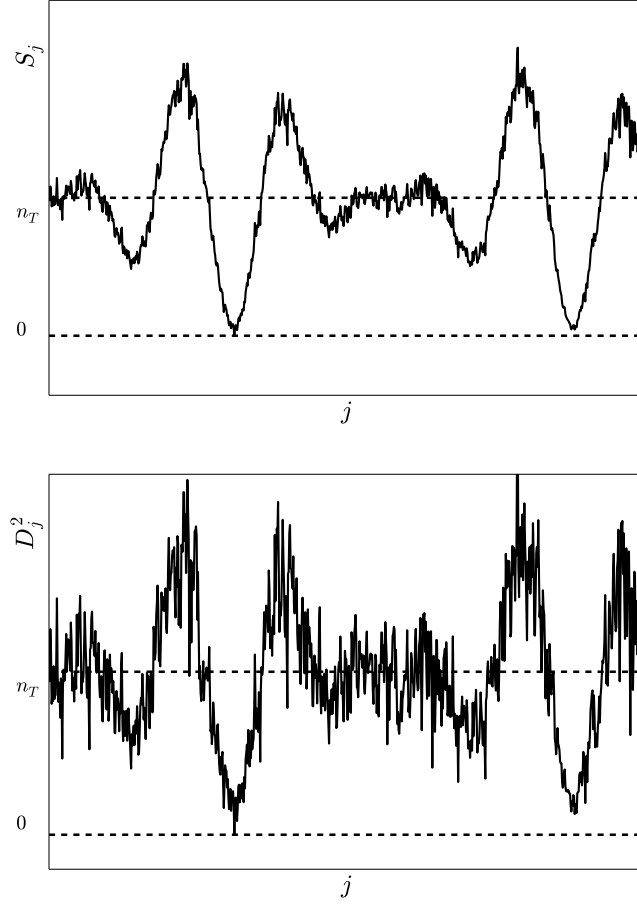


Fig. 1.— Theoretically expected noise characteristics of stationary thermal radiation as viewed directly and via a beam-splitter. Note the squared intensity difference still exhibits classical bunching noise that is correlated with the direct intensity time series. Additionally the former is also expected to have more shot noise.

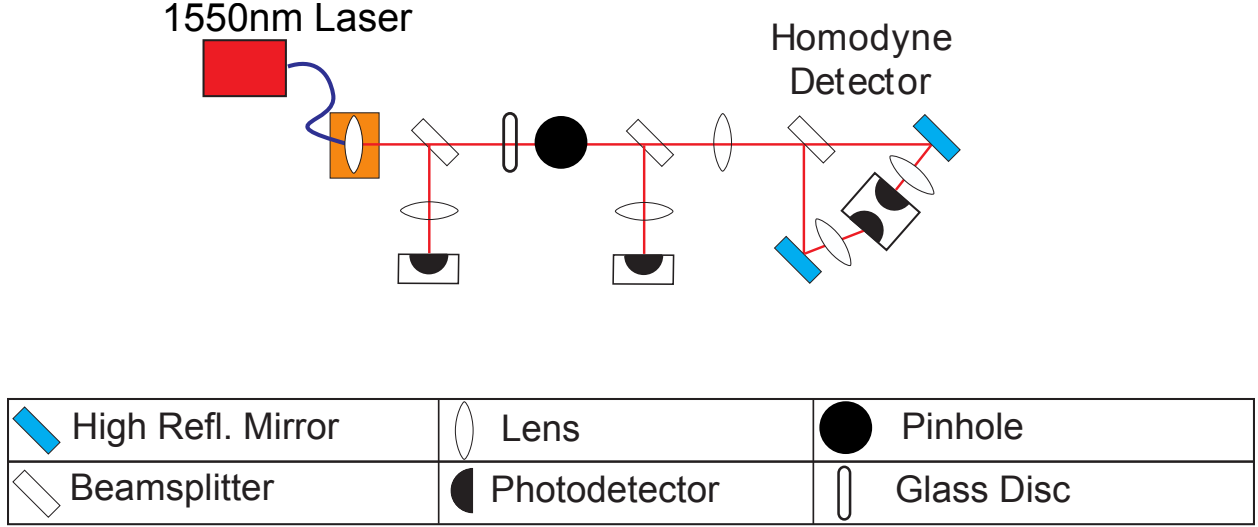


Fig. 2.— Experimental layout for the simultaneous flux measurements of a beam of coherent light . The ground glass is rotated off (optical) axis to produce pseudo-thermal light with classical bunching noise extending to $\sim 1 - 2$ MHz via scattering. The reflectivity of each beamsplitter is chosen such that the signal strength is optimised without saturating each detector.

The pseudo-thermal, or partially coherent, light generation is achieved by passing the output of the laser through a rotating unpolished glass disc as investigated by Martienssen (1964). The reason against enlisting a true thermal source for our setup is because the experiment needs to satisfy strict requirements on the detectors. Firstly, the light power has to be large enough that the shot noise of the field is measured well above the dark noise of the detector. Secondly, we have to be able to subtract any excess noise down to the shot noise level. Lastly, it is advantageous to be able to detect at frequencies above the photon bunching bandwidth. The rotating plate provides us the freedom to tune the excess (*i.e.* photon-bunching) noise bandwidth, through the rotation speed, such that the noise levels are suitable for the experiment.

The pseudo-thermal light so produced has a photon-bunching bandwidth of around 0.2 MHz, much less than the detector bandwidth of \sim approximately 50 MHz. The effect of the plate on the time and frequency domains can be seen in Figures 3 and 4 respectively. The technique can generate a pseudo-thermal state with coherence times down to 10^{-5} s. The state produced by the rotating plate has a relative amplitude of incoherent fluctuations

$$\nu = \frac{\sqrt{\text{var}(J_T(t))}}{\langle J_T(t) \rangle} \approx 0.15 \quad (1)$$

for flux measurements J_T performed in a sampling interval $T \ll \tau$, the coherence time, but

long enough to collect $\gg 1$ photons per interval (note that for fully incoherent light $\nu \approx 1$). The exact properties of the state produced by this method depend upon the focussing onto the plate, the rotation speed of the plate, and spatial filtering afterwards. The spatial filtering in our setup is done with the use of a $30\text{ }\mu\text{m}$ pinhole.

Next, we turn our attention to the three simultaneous detection schemes. The first beam splitter enables a flux measurement of a fraction (up to approximately $250\text{ }\mu\text{W}$) of the laser’s coherent laser light. Note that this occurs *before* the light has been affected by the rotating plate. The laser beam then passes through the rotating plate, after which there are two more beam splitters. The first one takes a direct detection of the pseudo-thermal light (the power of which is always equal to or greater than that detected by the homodyne detector). The final stage of the setup is a homodyne detection scheme of the pseudo-thermal light. At this stage, up to $200\text{ }\mu\text{W}$ is sent to a beam splitter, and the two output beams are then incident upon two photodiodes that enable a current subtraction, the benefits of which are discussed by Stefszky et al (2012). Figure 4 illustrates the limitation of the subtraction. It is seen that at low frequencies, below 0.5 MHz , the level of subtraction decreases. This is mainly due to the beam jitter effect that cannot be removed, because beam jitter modulates the photocurrent in each photodiode separately via the unique spatial dependence of the gain on the two photodiodes, Stefszky et al (2012). After the current subtraction the signal passes through an on-board 1.2 MHz high-pass filter and an external hardware 1 MHz high-pass filter. All of the signals are recorded simultaneously using an RTO1014 oscilloscope in which the direct and homodyne signals pass through a digital low-pass filter (DLPF) whose frequency is set to the appropriate frequency to remove aliasing in the Fourier transforms. Finally, it should be mentioned that all physical beams used for our flux measurements have high ($\gg 1$) photon occupation numbers.

2.2. Measurement strategy

In the homodyne detector, two photodiodes with up to $100\text{ }\mu\text{W}$ incident on each are connected before a transimpedance stage (gain of 20k followed by an output gain stage resulting in a bandwidth of around 6 MHz and up to 8 dB of dark noise clearance at 20 MHz), with one providing a positive current, and one providing a negative current when illuminated. In this way, the subtraction (of up to 60 dB) is done before the transimpedance stage of the detector and provides greater subtraction and stability as discussed by Stefszky et al (2012). The subtracted signal then goes through a 1.2 MHz high pass filter, an output gain stage and an external 1 MHz high pass filter before being measured at the oscilloscope. With this setup, however, one cannot simply take an addition measurement of the two fields incident on the two photodiodes. Instead, a separate detector takes a direct measurement in which the photocurrent passes through a transimpedance stage (with a gain of 2k , bandwidth

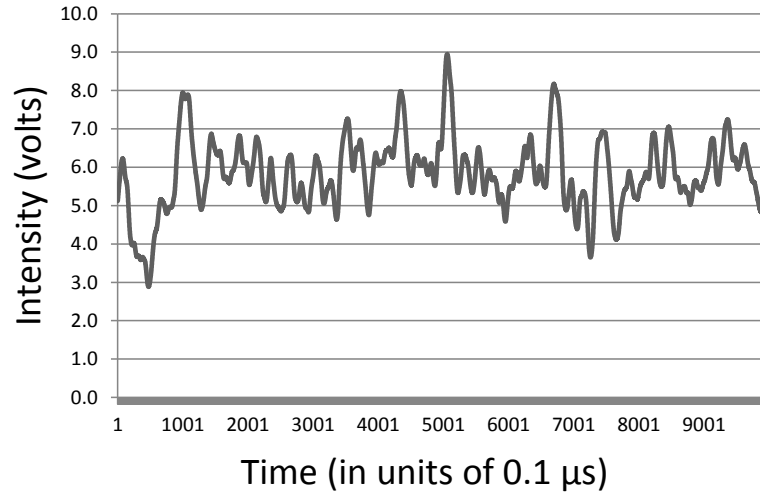


Fig. 3.— The time series of pseudo-thermal light as detected by the direct detection scheme, with the classical bunching noise generated by a rotating ground glass plate, see Figure 2.

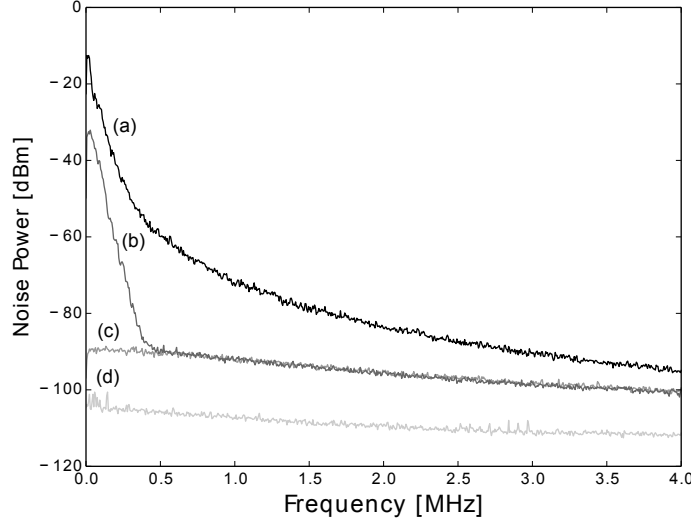


Fig. 4.— Spectra of the homodyne detector with different fields incident on the diodes showing typical characteristics of the fields. Trace (a) is the noise spectrum of the pseudo-thermal light (passing through the rotating plate), when all the incident power is on a single diode. Trace (b) is the pseudo-thermal light noise spectrum when the optical power is distributed equally between both diodes and subtraction is at a maximum. Trace (c) is when the rotating plate is removed and the power is equal on both diodes such that the shot noise of the coherent field is measured. Trace (d) is the dark noise of the detection system, whereby no light is incident on the detectors. Note that the incident power for traces (a),(b), and (c) are equal. All traces were taken with a spectrum analyzer with an RBW of 3 kHz and VBW of 10 Hz. Note also that for this measurement only, the gain of the detector is reduced from 20k to 2k.

of approximately 40 MHz) and then an output gain stage. On this detector, the maximum power before saturation is approximately 2 mW.

The oscilloscope is 4-channel so all measurements can be taken simultaneously. The oscilloscope settings were chosen to have the highest signal to noise for each measurement type and were not changed in between runs to ensure the noise floor of the oscilloscope does not vary. Note, however, that the noise floor of the oscilloscope is greater for the direct measurement due to the limited dynamic range of the device and the large amount of photon bunching noise. In the direct measurements, in which the signal was up to 10V in magnitude, the voltage noise from the scope has a mean of 0.025V and a variance of approximately $8\mu V^2$. Altogether three sampling frequencies f_s , all of which lie well above the bunching noise limit,

were adopted, where f_s is related to the time domain sampling interval T by

$$f_s = \frac{1}{2T}, \quad (2)$$

see Table 1 (note that because of the extra factor of two in the denominator of (2), f_s is actually the Fourier frequency of the detector rather than the sampling frequency in the usual sense). For each f_s there are multiple smaller data runs, whereby one full data run typically consists of six smaller runs of 40,000 samples per run. Here, the laser brightness was held constant (recorded using the reference beam) within each smaller data run, but stepwise decreased from one run to the next as illustrated in Figure 5. In the data analysis stage the extraneous low frequency noise in the homodyne subtracted time series (due to finite subtraction and beam jitter) was removed by Fourier transforming the signal and applying at the software level a heaviside high pass filter that excludes frequency components below 0.2 MHz. This was done by dividing the time series into many sets, each comprising 5,000 time contiguous samples; the resulting filtered spectra were then inverse-transformed back to the time domain and re-assembled to form the decontaminated HD signal, to be shown and discussed in the rest of the paper. Thus, in any comparison between homodyne (HD here-and-after) and direct measurements henceforth, *the HD time series data are already decontaminated*.

Sampling frequency f_s (MHz)	Sampling interval T (10^{-7} s)	Number of experiments	Number of runs per experiment
3	1.67	4	6
5	1.00	3	6
20	0.25	4 and 3	6

Table 1: Summary of measurements. Note that each run consists of 40,000 time contiguous samples. Also, as illustrated in Figure 2, the intensity of a fraction of the original coherent light is measured together with the remaining fraction that lost coherence after passage through the rotating glass plate; the intensity of the incoherent fraction of the light is further split into two parts, one is measured by direct detection and the other HD. All three intensities are simultaneously measured to form one cross comparing sample, and all sampling frequencies lie well above the bunching noise limit. The laser flux is stepwise reduced from one experiment to the next in the manner shown in Figure 5. Note that for 20 MHz two acquisitions were taken, one with 4 experiments and the other 3, *i.e.* the periodic structure of the pedestal in Figure 5 is repeated 4 times in one acquisition and 3 in another.

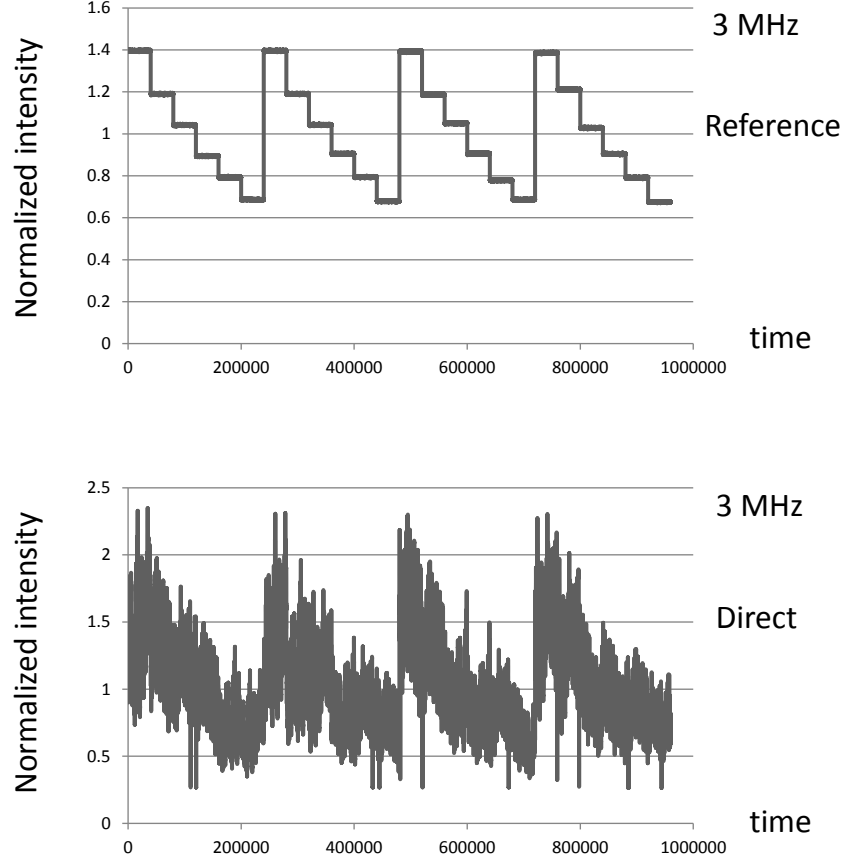


Fig. 5.— Combined intensity variation pattern of the laser light for a full data run with no change of beam alignments and other hardware arrangements between experiments (top). The interval between consecutive samples is 1.67×10^{-7} s, corresponding (by (2) and Table 1) to a sampling frequency of 3 MHz. Each ‘tooth’ of the pedestal time series spans 40,000 samples, and this applies to other sampling frequencies as well. The bottom graph shows simultaneous intensity measurement, by the direct method, of a fraction of the laser light that became partially incoherent when it passed through the rotating glass plate (see Figure 2). All intensities shown are normalized to a mean of unity over the entire time series. The increase in the variance w.r.t. the coherent time profile (top) will be used as a gauge of the level of extra noise in the absolute measurement of the incoherent flux.

3. Correlation analysis

We are now ready to discuss the central part of the test: autocorrelation (ACF) data. At each of the four sampling frequencies, the time series of the laser reference, direct, and HD measurements (the first two are shown in Figure 5 for the 3 MHz case) are simultaneously compared in this test. But firstly, we wish to remind the reader of the theoretical ratio of the covariance to the square of the mean for stationary light. Thus, if the light is fully incoherent with a Gaussian ACF peak of the form e^{-t^2/τ^2} , eq. (32) of Lieu & Kibble (2015b) indicates that for the homodyne squared difference current it is

$$\frac{\text{cov}(D_k^2, D_l^2)}{\langle D_k^2 \rangle^2} = e^{-t_{kl}^2/\tau^2} + 4\delta_{kl}; \quad (3)$$

and for the directly detected current (9) leads to

$$\frac{\text{cov}(J_k, J_l)}{\langle J_k \rangle^2} = e^{-t_{kl}^2/\tau^2}, \quad (4)$$

where in both equations $\text{cov}(A, B) = \langle AB \rangle - \langle A \rangle \langle B \rangle$ with $\langle \dots \rangle$ denoting ensemble mean, $t_{kl} = (k - l)\tau$ and τ is the inverse bandwidth of the incoherent light (assumed to have a Gaussian spectrum). If the light is partially incoherent, as is the case here, the two ratios would become

$$\frac{\text{cov}(D_k^2, D_l^2)}{\langle D_k^2 \rangle^2} = \nu^2 e^{-t_{kl}^2/\tau^2} + 2(1 + \nu^2)\delta_{kl}; \quad (5)$$

and

$$\frac{\text{cov}(J_k, J_l)}{\langle J_k \rangle^2} = \nu^2 e^{-t_{kl}^2/\tau^2} \quad (6)$$

respectively, where ν is the relative amplitude of incoherent fluctuations as defined in (1).

Since $\nu \ll 1$, the ACF of the square HD time series (*i.e.* the decontaminated measurement of D_j^2) should have (a) a sharp central spike of magnitude ≈ 2 , dropping rapidly to assume (b) the Gaussian function of the classical bunching noise in the direct current autocorrelation, although we emphasize that we actually never measured a clean Gaussian in either the ACF of the direct or squared HD time series, but a central broad peak and a long tail because of the existence of long range correlations in the bunching noise of the incoherent light we used. Moreover, although the light signal we used is explicitly time varying, *viz.* it is periodic (having the pedestal time series of Figure 5 due to varying the laser output power), this non-stationarity occurs on very long timescales and does not grossly distort the small lag features of (5) and (6), but only further extends the (already long) tail of the ACF beyond that of the classical bunching noise.

Turning to the graphs, it should be stated upfront that the aforementioned sharp central spike was *always* detected in the squared HD time series (*viz.* the decontaminated measurement of D_j^2), and because this shot noise effect is insignificant when many samples are averaged, we will not show the spike. Rather, by avoiding the central two bins of the ACF data, we could reveal much more clearly what really matters, the much broader (than the shot noise) peak of the classical bunching noise. In this respect we find, surprisingly, that apart from the ignored small lags the ACF of the HD signal lies *beneath* the direct; moreover, the higher sampling frequency data have a greater difference between the direct and homodyne measurement results. In Figure 6 we show the behavior in two such frequencies, 3 and 20 MHz, where the ACFs of the direct, HD squared, and source (laser) reference fluxes are all seen. Note the manner in which the residual HD shot noise spill-over at small lags quickly gives way to the bunching noise correlation (which is absent in the coherent laser signal, the long ACF tail there is entirely due to the periodic variation of the intrinsic laser power – the pedestal of Figure 5 – recalling that even 30,000 samples covers only 3/4 of a single laser power pedestal), but for the incoherent light of the other two traces this correlation power is *smaller* in the case of the HD than the direct. In fact, the ACF tail of the HD gradually merges with the intrinsic effect of the reference signal’s variation, indicating that the HD process significantly reduced the correlation power of the bunching noise in the partially coherent light, while preserving the intrinsic variation of the original laser flux. Note also that the width of the bunching noise peak, *viz.* the tail after the initial drop, is less for the 20 MHz run, indicating that (unlike the period of the reference signal variation, which is only constant in terms of the number of samples) the bunching noise coherence length is very crudely a constant, independent of the timing resolution of the data.

4. Variance as a function of sample size

From the viewpoint of sensitivity of intensity measurements, the performance of the direct and HD methods must be compared in terms of the variance for a given sample size. This figure of merit is computed by bin-averaging the time series data, using a fixed number of samples N per bin (for stationary light, the ensemble average of the result equals the sum of the covariance over all lags between 0 and N , divided by N). The relative variance of the binned series, defined as the ratio of the variance to the square of the mean, may then be plotted against N . This is shown, for the 3 sampling frequencies we adopted, in Figures 7 to 10, where the constancy of the reference signal trace is due again to its periodic variation but the excess variance of partially incoherent light detected by the HD and direct methods is due to the bunching noise.

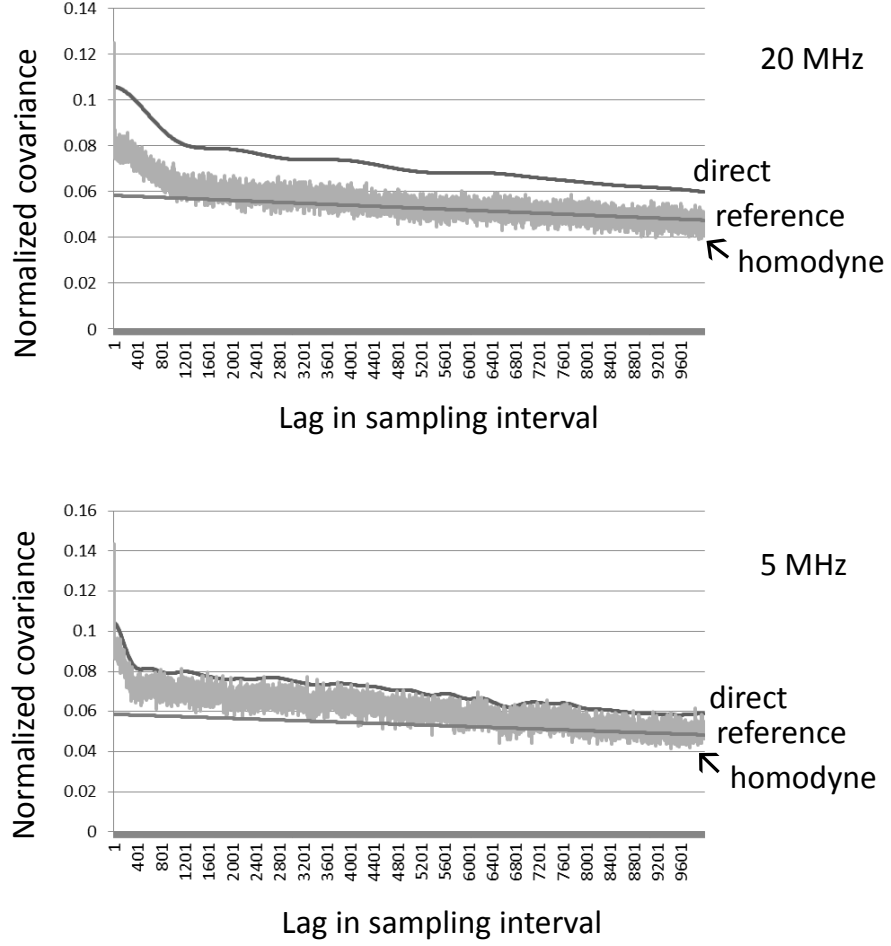


Fig. 6.— The ACF measurements of the direct, HD squared (lightest color), and reference signals for two sampling frequencies. The normalized covariance is defined as the covariance divided by the product of the means, *i.e.* $\text{cov}(A, B) / \langle A \rangle \langle B \rangle$ where $\text{cov}(A, B) = \langle AB \rangle - \langle A \rangle \langle B \rangle$ and the ensemble mean $\langle \dots \rangle$ is estimated by the sample mean. Each series consists of 960,000 samples as can be inferred from Table 1 and its caption. The central two lag intervals are omitted from all data to avoid the very tall shot noise peak in the HD squared signal (there is still some spill-over into the next several bins, resulting in the much shorter spike on the extreme left). The suppression of the ACF power of the HD squared relative to the direct signal is evident in most lags, and indicates the HD process reduces bunching noise.

The noise variance so inferred is plotted in the lower graph of each figure, where we included the performance of the (unattainably idealized) HD method as envisaged in Lieu et

al (2015a), to highlight that HD did not completely remove the bunching noise to reach the shot noise limit of Lieu et al (2015a). Nevertheless, the ratio of the direct noise variance to the HD as a measure of the sensitivity improvement does become quite large as N exceeds 500 and the shot noise in the HD squared time series is ironed out by the bin averaging. In Figure 12 we show how, at the fixed N value of $N = 800$, this ratio changes with sampling frequency, as there appears to be the expected rising trend. We also show in Figure 11 how the two time series actually look when they are binned to $N = 800$. With the reference data of Figure 5a in mind, it can be seen that the HD method did remove some of the incoherent noise to ‘recover’ the original pedestal shape. In fact, a least square test revealed that Figure 11b has a smaller χ^2 difference from Figure 5a than Figure 11a by $\approx 25\%$, although the absolute values of these two reduced χ^2 are not so important because they are subject to the systematic effect of the large timescale uncertainty in the incoherent flux as measured by either of the two methods.

5. Discussion and conclusion

We performed a detailed experimental investigation comparing the performance of direct versus HD measurement of the flux of incoherent light, with the latter inferring the flux from the shot noise variance of the light. The experimental results showed that the HD method, as originally envisioned by Lieu et al (2015a), did result in an improvement in accuracy w.r.t. the direct detection. This is contrary to the expected theoretical behavior predicted by Lieu & Kibble (2015b); Nair & Tsang (2015); Zmuidzinas (2015).

Specifically, the most surprising result of our experiment is seen when comparing Figure 11 with Figure 5a. It is evident that the direct detection of Figure 11a has two kinds of time variability, *viz.* (a) the intrinsic and periodic pedestal signal of the coherent laser source; and (b) the incoherent fluctuations superimposing upon the pedestal, that emerged after the laser light passed through the rotating glass plate. As Figures 11b and 7 through 10 showed, for the *same* bin size of running average the HD detection method preferentially reduced *only* the incoherent variations. From these results, it would appear as though the HD is able to distinguish incoherent thermal fluctuations at constant brightness temperature from those that involve a genuine intrinsic change in brightness (via the change in the underlying laser power).

The most obvious question is whether some overlooked element of the experiment that led to a misrepresentation of the theoretical ansatz could explain the discrepancy between predicted and observation. This has also got to occur in the form of some difference between the two detection methods that offered an evasive advantage to the HD, when any such

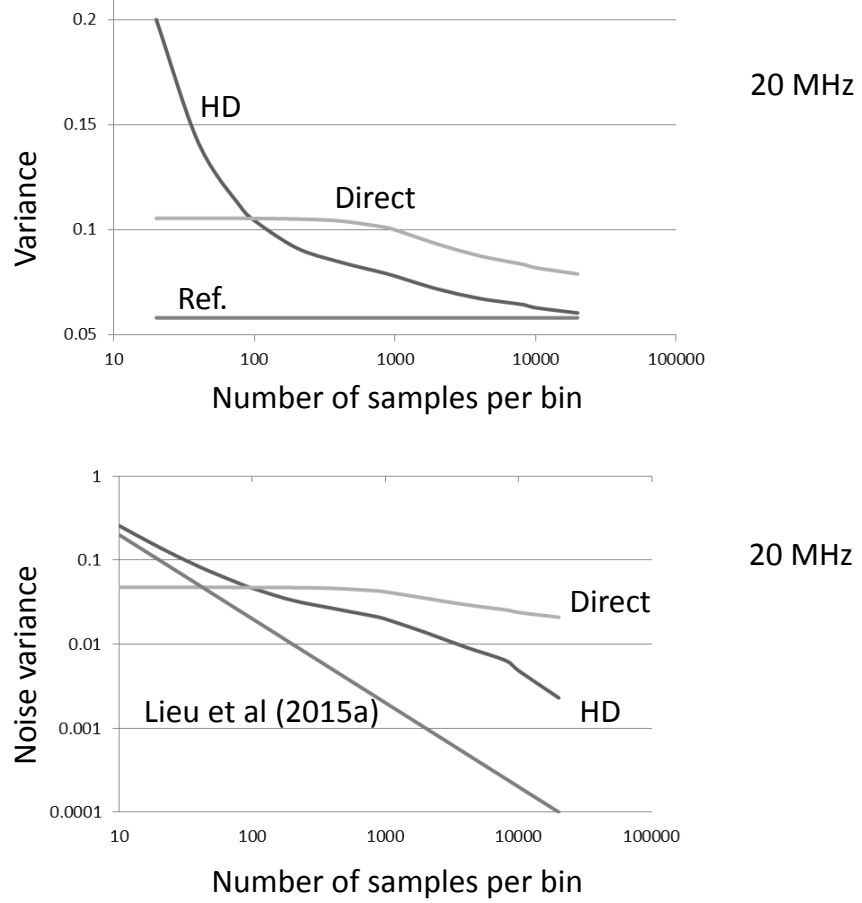


Fig. 7.— Variance in the direct and HD detected time series, both sampled at the rate of 20 MHz, as binned into various sizes. The intrinsic laser source effect is also included for comparison. Note that the excess variances above the laser value are due to the bunching noise in the HD and the direct signals. This noise variance is plotted in the lower graph where the bottom curve depicts the homogeneous shot noise limit of $\approx 2/N$ for the HD variance as predicted by Lieu et al (2015a), *viz.* the δ_{kl} term in (5). This limit is obviously unattainable.

effects would in general do the opposite because the HD method is more complicated and susceptible to extra noise contamination. One difference between the two is the filtering, and one might ask if the high pass filter that removed the stray low frequency HD noise might (section 2.2) be the responsible cause of the improvement. The answer is a prompt ‘no’, and is already provided by Nair & Tsang (2015), who showed that quantum field theory

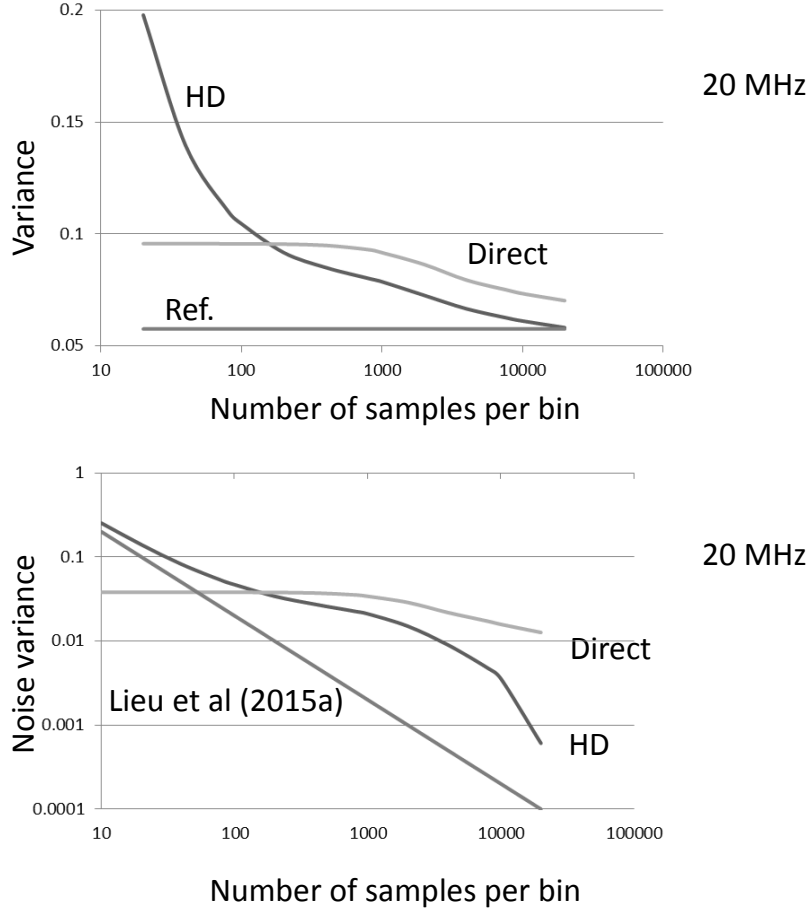


Fig. 8.— As in Figure 7, except for an independent data set of 720,000 samples acquired also at the rate of 20 MHz (in Table 1, this refers to the acquisition involving 3 experiments with 6 runs per experiment).

imposes a strict lower bound to the noise, at the level of the direct detection. Moreover, Lieu & Kibble (2015b) also showed that spectral filtering of the subtracted HD time series cannot result cause the HD accuracy to surpass the direct. The other possibility for the discrepancy between the experimental results and the theory is that a truly incoherent light source was not used, although this too is a long shot explanation because of the universal bound of Nair & Tsang (2015), which applies to all forms of light.

To further investigate this interesting and potentially very important anomaly, we emphasize that the incoherent noise has a much higher frequency than the pedestal variation

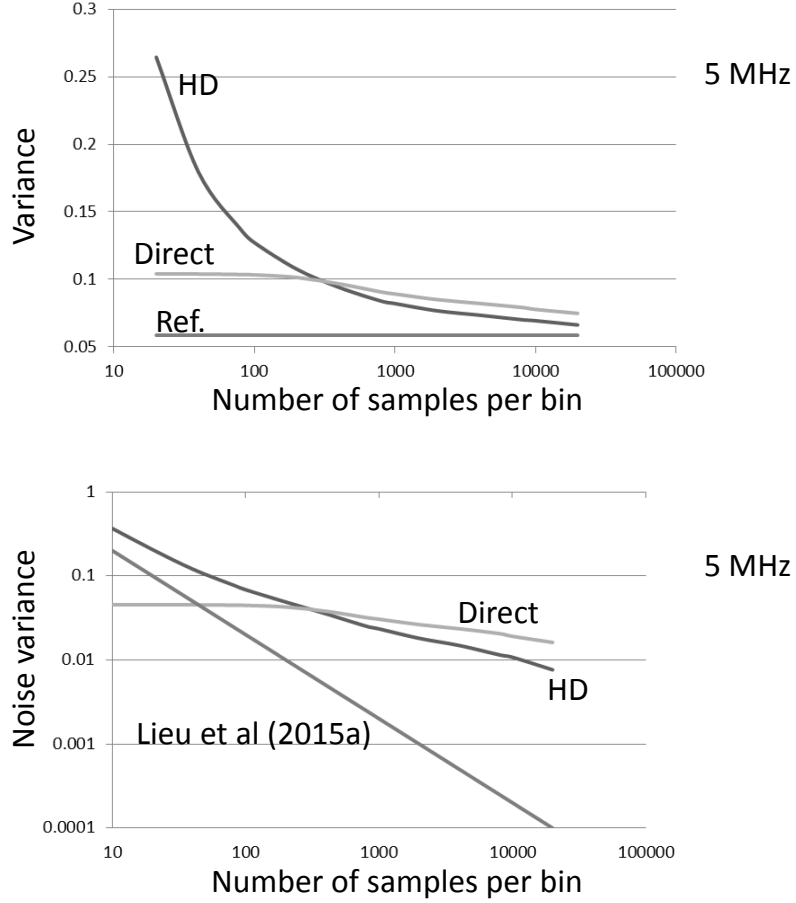


Fig. 9.— As in Figure 7, except for an independent data set of 720,000 samples acquired at the rate of 5 MHz (see Table 1).

of the laser power, as is noted in Figure (5). Thus, to remove or reduce the low frequency pedestal power fluctuations one should be enlisting the very opposite frequency selection criterion, *viz.* a low pass filter. This conclusion is also apparent in the top half of Figures 7 – 10, where it is seen that as the bin size increases the variance of the direct and HD fluxes decreases while the reference signal hardly changes, because the last is only affected by the incoherent fluctuations. As mentioned previously, both the direct and homodyne detection signals pass through the same low-pass filter in the scope. The other way to invoke a low pass filter is to average the flux over a larger bin size. However, provided one compares the direct and HD performance using the *same* bin size, no such clean-up process could preferentially have been applied to one data set more than the other. Yet this is precisely how our

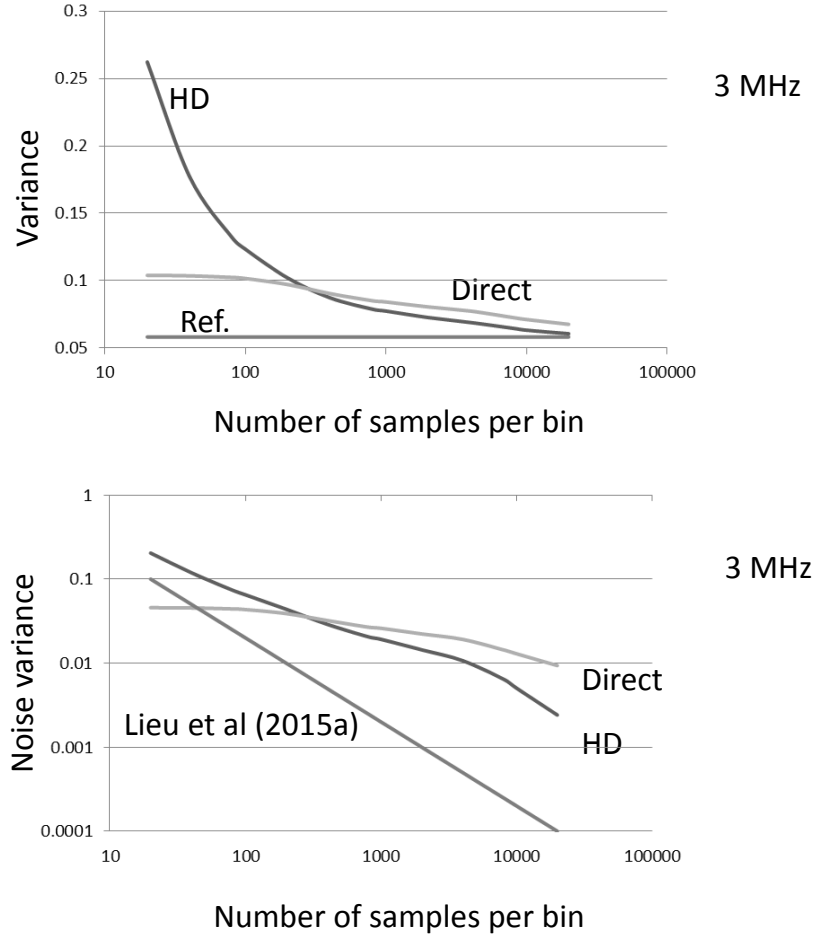


Fig. 10.— As in Figure 7, except for an independent data set of 960,000 samples acquired at the rate of 3 MHz (see Table 1).

comparisons were made.

Although our experiment explored the more general scenario of non-stationary light (because of the way in which the variations of the laser power, *viz.* the pedestals) which Lieu & Kibble (2015b); Zmuidzinas (2015) did not address, Nair & Tsang (2015) provided a robust proof, based upon the Cramer-Rao bound of quantum estimation theory, that the HD method fundamentally cannot be more sensitive than direct detection under any circumstance. Thus there *is* a conflict between theory and experiment. In fact, the results here also appear to be at odds with Nyquist theorem, which states that in the case of high photon occupation number beams one cannot hope to retrieve additional information

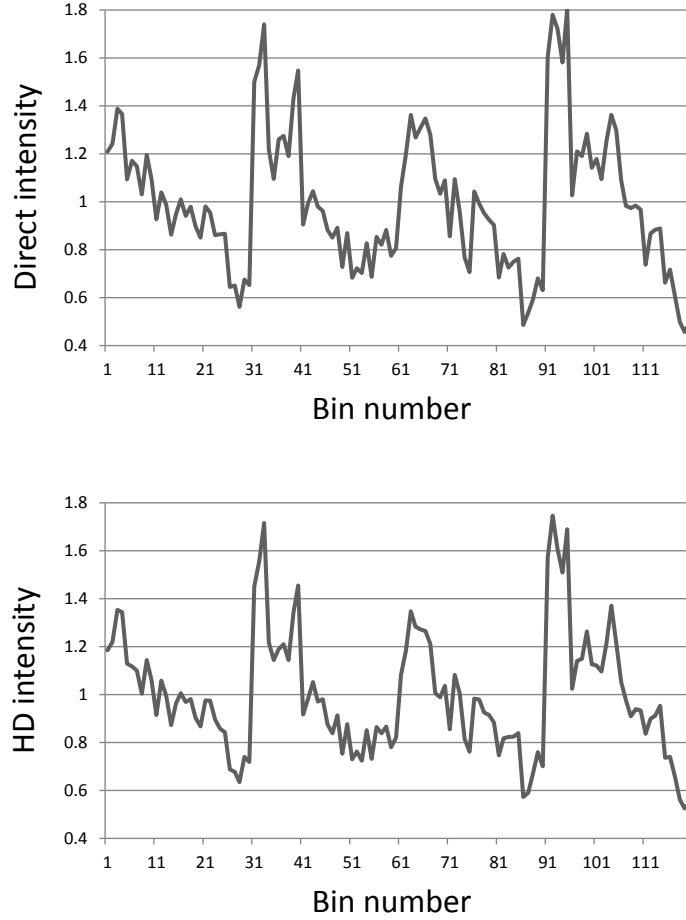


Fig. 11.— The direct (top) and HD (bottom) time series sampled at the frequency of 20 MHz, and bin-averaged every 800 (*i.e.* $N = 800$) of the 960,000 samples of the first acquisition in Table 1. The HD time series is obtained after the Fourier transform, filtering and then inverse Fourier transform. The two series are to be compared to the underlying pedestal shape of the coherent reference signal, Figure 5. Although Figure 5 showed data sampled at 3 MHz, the shape is identical to the 20 MHz case here; moreover, the bin averaging performed here does not distort the shape because 800 samples occupy a small fraction of each ‘tooth’ of the pedestal (which comprises 40,000 samples). The χ^2 difference between the direct and the reference time series is approximately 25 % higher than that between HD and reference (the former is $\chi^2_{\text{red}} = 0.021$ and the latter is $\chi^2_{\text{red}} = 0.017$, both for 119 degrees of freedom).

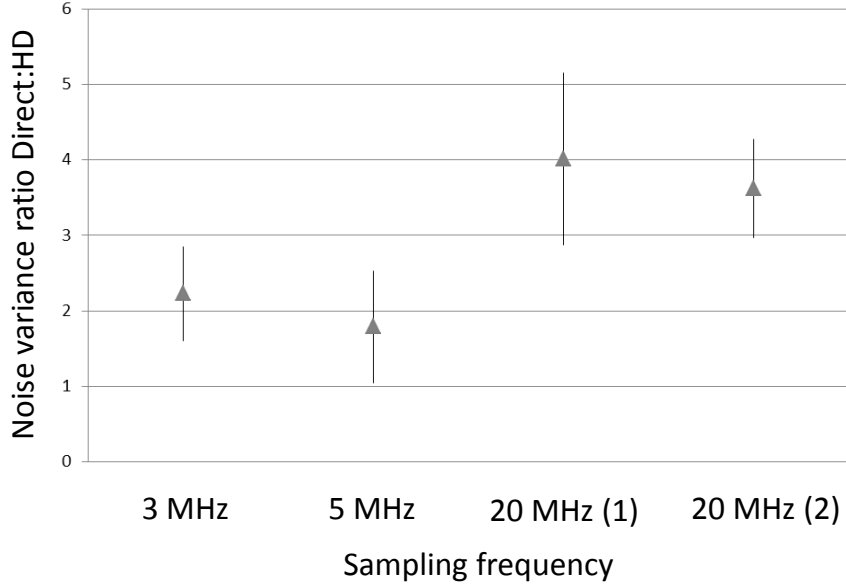


Fig. 12.— The ratio of the bunching noise variance, direct to HD, in the case when the time series were bin-averaged every 800 (*i.e.* $N = 800$). The error in the ratio is obtained by computing the variance in this ratio from the data.

about the signal by sampling more frequently than the coherence time of the bunching noise, *i.e.* the signal-to-noise ratio will not increase beyond the limit of the radiometer equation. Since our sampling time T is always smaller than the coherence time of the fastest bunching noise component, and the sensitivity improvement appears to be more pronounced when T is decreased, Figure 12, this means that when rapid sampling was applied in conjunction with HD detection, it would appear that one *can* surpass the radiometer equation.

At this point we cannot offer a theoretical explanation of why the HD method outperformed the theoretical expectation of Lieu & Kibble (2015b); Nair & Tsang (2015);

Zmuidzinas (2015). What we have presented is robust evidence that the experimental setup as described showed unambiguously a homodyne detector measurement tracking more accurately the input flux than the direct measurement. Because of the ramifications of this result, an understanding of the conditions that made this effect possible is vital. If the effect is intrinsic to the HD measurement process it will have far reaching consequences, as the results of the higher order quantum field theory described by Zmuidzinas (2015); Lieu & Kibble (2015b); Nair & Tsang (2015) would then be called into question.

REFERENCES

- Fox, M., 2006, Quantum Optics, p94-98, Oxford
- Lieu, R., Kibble, T.W.B., & Duan, L., 2015, Ap.J. 798, 67
- Lieu, R., and Kibble, T.W.B., 2015, Proc. of the 26th Symp. on Space Terahertz technology, paper W2-3 ((arXiv:1509.01868)
- Martienssen, W. & Spiller, E., 1964, Coherence and fluctuations in light beams, Am. J. Phys., 32, 919
- Nair, R., and Tsang, M., 2015, ApJ, 125, 6
- Shen, Y., Tien, L., Zou, H., 2010, PRA, 81, 063814
- Wang, L.J., Magill, B.E., & Mandel, L., 1989, J. Opt. Soc. Am., 6, 964
- Zmuidzinas, J., 2015, Ap.J., 813, 17
- Stefszky, M.S., & Mow-Lowry, C.M., & Chua S.S.Y., & Shaddock, D.A., & Buchler, B.C. & Vahlbruch, H., & Khalaidovski, A. & Schnabel, R. & Lam, P.K., & McClelland, D.E., 2012, Class. Quantum Grav., 29, 145015.